Impact of Silicone Gel Breast Prosthesis on Post-Mastectomy Photon Beam Therapy of a Recurrent Carcinoma

Ramaesela Welhemina Letsoalo[1*], Mpho Enoch Sithole[2], Mpumelelo Nyathi[1]

1. Sefako Makgatho Health Sciences University, Department of Medical Physics, P. O. Box 146, MEDUNSA, Pretoria, 0204, South Africa
2. Sefako Makgatho Health Sciences University, Department of Physics, P. O. Box 98, MEDUNSA, Pretoria, 0204, South Africa

A R T I C L E I N F O	A B S T R A C T
	Introduction: Silicone gel breast implants are used for breast reconstruction after mastectomy. In case of cancer recurrence, the radiation oncologists are forced to irradiate through the prosthetic device, which leads to the incidence of dose perturbations during the treatment due to the high atomic number of prosthesis. Regarding this, the present study aimed to investigate the influence of silicone gel thickness on photon beam distribution. ***Material and Methods:*** A VARIAN linear accelerator, water phantom (dimensions of $30\times30\times30$ cm^3), silicone gel breast prosthesis, and Omni-Pro Accept software were used. Gantry positioned at $0°$ and a source-to-surface distance of 100 cm, the collimators adjusted to a field size of 10×10 cm^2 and photon beam energy of 6 MeV was used. The results obtained with a MCNP Code were validated with the measured data. The beam profiles and PDD curves were also measured for silicone gel thicknesses of 4, 6, 8, 10, 12, 14, and 16 cm with the width of 16.5 cm aligned 1 cm below the water surface. ***Results:*** According to the results, the measured and calculated percentage depth dose ratio was ≤ 0.03. Furthermore, the measured and calculated beam profiles were 0.5% and 0.9%, respectively. For the silicone gel prosthesis, the depth dose values at 0.5 cm below the prosthesis were $\leq 2.8\%$. ***Conclusion:*** As the findings indicated, dose perturbations below the breast prosthesis were insignificant. Therefore, breast prosthesis could be concluded to be safe in case of carcinoma recurrence.

Introduction

Breast cancer is regarded as a common cause of cancer death amongst women worldwide. The breast cancer is on a growing trend in the lower-income countries, which has accordingly increased the rate of mortality in these regions [1]. Surgery is the main therapeutic option for breast cancer, which is accomplished by tumor localization. This treatment is then followed by chemotherapy, radiotherapy and adjuvant hormonal therapy.

According to the literature, the use of adjuvant radiation therapy following mastectomy for breast cancer is a beneficial approach. However, post-mastectomy radiation therapy is still a controversial issue, which has not been investigated sufficiently [2]. Based on the evidence, the local recurrence of stages I and II breast cancer has the prevalence rates of around 10% and 15%, respectively [3].

Breast reconstruction is a type of surgery performed on women who had undergone mastectomy [3]. Concerns have been raised over the effect of silicone gel prosthesis on the delivery of radiation treatment in cases with breast cancer recurrence [4]. Surgery facilitates the reconstruction of the breast with the same size and shape as it was

before removal [5, 6]. Breast reconstruction can be accomplished through several types of operations.

The most commonly used prosthesis is a saline-filled prosthesis, which is a silicone shell filled with salt water. Silicone gel-filled prostheses are another option for breast reconstruction [7]. Nonetheless, the use of these prostheses was prohibited due to concerns over silicone leakage that might results in other breast side effects affecting the immune system [8-11].

Radiation therapy, involves delivering the exact amounts of high-energy radiation to eradicate malignant cancer cells. In a study conducted on the radiation effects on silicone gel and radiation dose distribution through breast prosthesis, it was observed that silicone gel behaved like tissue and that its half-value thickness and density were comparable to that of water. In the mentioned study, dose distributions in and under the silicone gel breast prosthesis were reported to have little alteration when irradiated with ^{60}Co and 4 MeV photon beams [12].

However, the use of 150 keV to 15 MeV photon beams resulted in no significant alteration of depth

Corresponding Author: Tel: +27125214380; Email: welhemina.letsoalo@smu.ac.za

dose away from the silicone gel prosthesis with minor interface perturbations [13, 14]. In another study, at the depths lower than the practical range of the electron beams (i.e., 9-20 MeV) the measured dose distribution showed no significant difference in the dose delivered in the presence of the silicone gel prosthesis [15].

The aim of radiotherapy is to maximize the dose applied to the tumour below the silicone gel prosthesis while keeping the dose to the tissue as low as possible. It was recommended to avoid passing the radiation beam through a prosthetic device before reaching a target volume [16]. However, this is not always possible in cases, such as silicone gel breast prosthesis. With this background in mind, the present study was conducted to investigate the impact of silicone gel thickness on dose distribution below the prosthesis when irradiated with 6 MeV photon beams. Calculations were performed in region directly below (i.e., distal region) the prosthesis using Monte Carlo method.

Materials and Methods

Experimental setup

The measurements were performed using a Varian 2100C linear accelerator (Varian Oncology Systems, Palo Alto, CA) equipped with multileaf collimators (MLCs) with the nominal photon energy of 6 MeV. All measurements carried out in a $30\times30\times30$ cm^3 water phantom (PTW-Freiburg, Germany) positioned beneath the linear accelerator gantry at an angle of 0° as indicated in figure 1. The wall built-in lasers were used to align and position the water phantom.

A source-to-surface distance (SSD) of 100 cm was determined for the measurement of depth dose and profile distribution. The SSD was set at the surface of the water with the aid of an optical distance indicator embedded inside the gantry head. The MLCs were adjusted to give a reference field size of 10×10 cm^2 so that the light beam strike on the centre of the field (central axis [CAX]) following the jaws orientation inside the gantry.

The PTW ionization chamber (PTW, *Freiburg*, Germany) was aligned to be at the centre of the field, and its motion was enabled by the connection of the linear current booster motor cable to the local control port on the water phantom. The orientation (x, y, z) of the phantom was considered during the alignment as shown in figure 1. The RFA MCU Scanditronix Wellhőfer (*Freiburg*, Germany) control unit cable was used for the connection to the water phantom serial port.

The RS323 cable (*Freiburg*, Germany) was also connected from the control unit to the computer installed with the Omni-Pro Accept software (*Schwarzenbruck*, Germany) for plotting percentage depth dose (PDD) curves and the beam profile curves. The detector orientation was tuned to produce the maximum spatial resolution for both dose profile and depth dose measurements in the x- and y-directions, respectively.

The reference diode was also aligned in a fixed position in the field to monitor the beam intensity with time without obstructing the beam. The ionization chamber was adjusted to move in a water phantom to sample the dose rate at various points whereas the reference diode remained fixed throughout the measurements. The coordinate system [(x, y, z)=(0, 0, 0)] was located at the front surface of the target where the electrons were incident. The isocenter of the accelerator was defined at (x, y, z)=(0, 0, 100). The linear accelerator was set to apply 100 monitor units (MU) per minute.
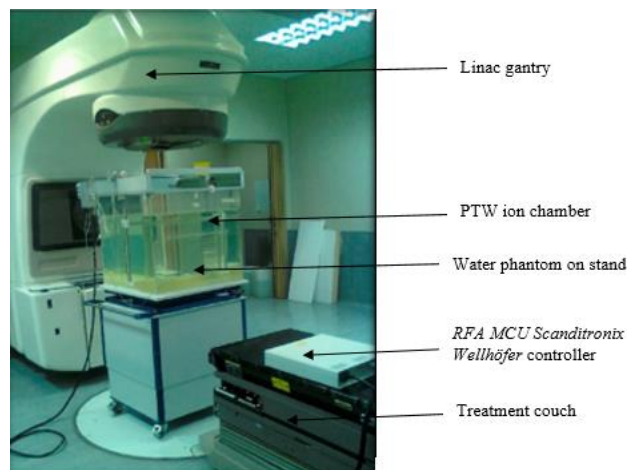
Figure 1. Experimental setup used to measure profile and depth dose data [17].

Measurements

Measurements were carried out using a 0.6 cc ion chamber for dose distribution under the same conditions as indicated in section 2.1. Depth dose were scanned using a three-dimensional (3D) scanning water phantom system (RFA-300, *Scanditronix, Wellhofer, (Freiburg*, Germany). The chamber in the phantom was positioned at the SSD of 100 cm.

Silicone gel breast prostheses (*Du Plessis Orthotics & Prosthetics*, South Africa) were immersed in water. The top surface of the prosthesis was aligned 1 cm below the surface of the water in the phantom. The dose profile and depth dose measurements in water were performed with and without the silicone gel breast prosthesis in place. The measurements were repeated three times under the same condition. The measured data were normalized to 100% at CAX.

Monte Carlo simulation

The radiation transport of photons was simulated using the Monte Carlo Nuclear Particle (MCNP) code. This code simulates various 3D geometries using voxels. The code is capable of simulating photon interactions with matter through the user-defined geometry and material compositions. The detailed description of the software can be found in Shultis *et al*, [18]. Figure 2 illustrates the schematic diagram of MCNP simulated water phantom.

The voxel was built as a combination of several predefined surfaces. Every voxel (volume element) was

assigned a material according to the arrangement in the phantom. A sequence of voxel was used to form a water phantom with layers of water and silicone gel. The simulation phantom was built from 0.2×0.2×0.2 cm voxels in any direction. The voxels representing the various thicknesses of the silicone gels were generated using the surface and cell cards commands. The cell cards commands were defined for the densities of different materials, such as dry air, water, and silicone gel in grams per cubic metre (g/cm^3).

The MCNP input geometry file was comprised of several surface cards, cell cards, and data cards. The 30×30×30 cm^3 water phantom was simulated on a Linux-based operating system. The interior parameters of the water phantom were defined to enable calculations for both radial (PZ +101, +102, …, +129) and axial (CZ +0.5, +1.5, …+10.5) distributions of the dose. The 10×10 cm^2 field size at the SSD of 100 cm was defined by using the data cards.

The cell flux tally was identified for the voxels in which the particle scoring was expected and the energy bins were created for the deposition of dose. The sum of the photon fluence contribution was reported in the MCNP output file for plotting the PDDs and beam profile data. The produced output data file included geometry specifications such as voxels in all directions and their boundaries, together with the dose values and statistical uncertainties (1σ) in the individual voxel. The statistical uncertainty in the dose was generally 2%.

In this study, we used 6 MeV photon beam of a Varian 2100C linear accelerator. The linear accelerator materials and dimensions were incorporated based on the manufacturer's specifications. The incident beams coming from the exit window of the linear accelerator were modelled as a point source with a radius of 0.2 cm. During simulation, the electron cut-offs energy (ECUT and AE; kinetic+rest mass) and photon cut-offs energy (PCUT and AP) were 700 and 10 keV, respectively. The numbers of particle histories were $2.0×10^7$ and $3.0×10^7$ in the electron and photon files, respectively.

Silicone gel prosthesis properties

The general properties of silicone include low thermal conductivity, low chemical reactivity, low toxicity and thermal stability, as well as high moisture and heat-resistance [19]. Silicone gel breast prosthesis is characterized by a thin silicone containing a soft, transparent, thick, and sticky gel, which closely mimics the feel of a human fat [20]. Silicone gel breast prosthesis used in this study consists of polydimethylsiloxane [(CH$_3$)$_2$SiO]$_n$ with physical density of 0.97 g/cm^3 and effective atomic number of

10.37 [21]. In this study, seven silicone gel breast prostheses of different thicknesses (i.e., 4, 6, 8, 10, 12, 14, and 16 cm) were used. All silicone gel prostheses had the width of 16.5 cm. In all setups, the surface of the prosthesis was aligned 1 cm below the surface of the water.
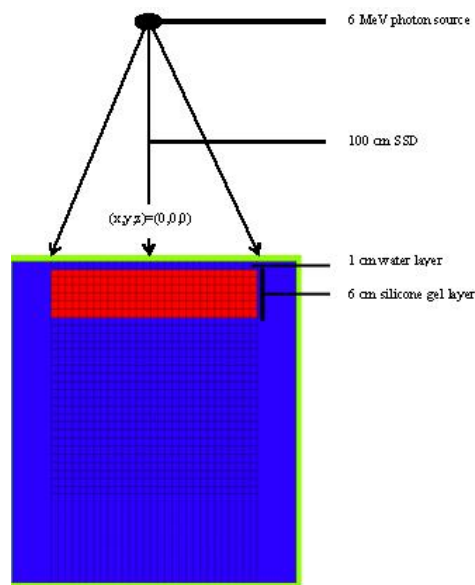
Figure 2. A two-dimensional Monte Carlo Nuclear Particle code simulated water phantom with a photon source directed at the source-to-surface distance of 100 cm

Validation of the accelerator model

The calculated PDDs and beam profiles were then compared to the measured data. The accelerator model was fine-tuned to adjust the parameters as described in the literature [22, 23]. The radial intensity and the mean energy for electron beam were adjusted until the beam profile, PDD, and measured data were within the acceptance value.

Results

Measurements

Figure 3 depicts the experimental percentage depth dose for various sizes of silicone gel for 6 MeV photon beams in water phantom with a 10×10 cm^2 field size defined at the SSD of 100 cm. All curves were normalized to the maximum dose in water along the CAX.
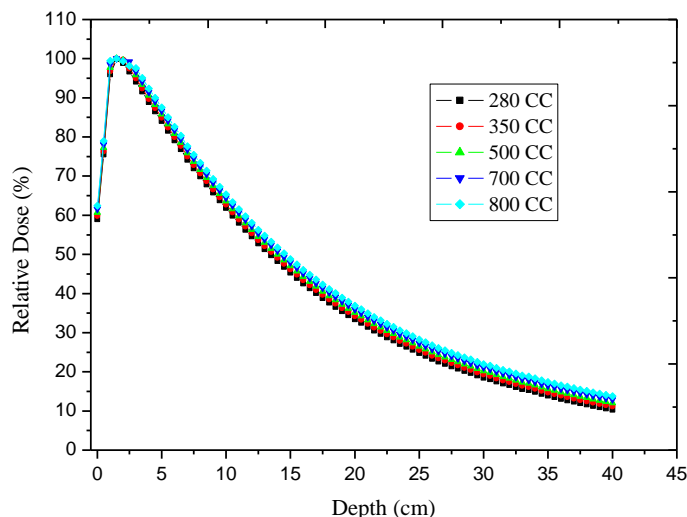
Figure 3. Comparison of measured depth dose distribution for 6 MeV photon beam with the field size of 10×10 cm^2 defied at source-to-surface distance of 100 cm
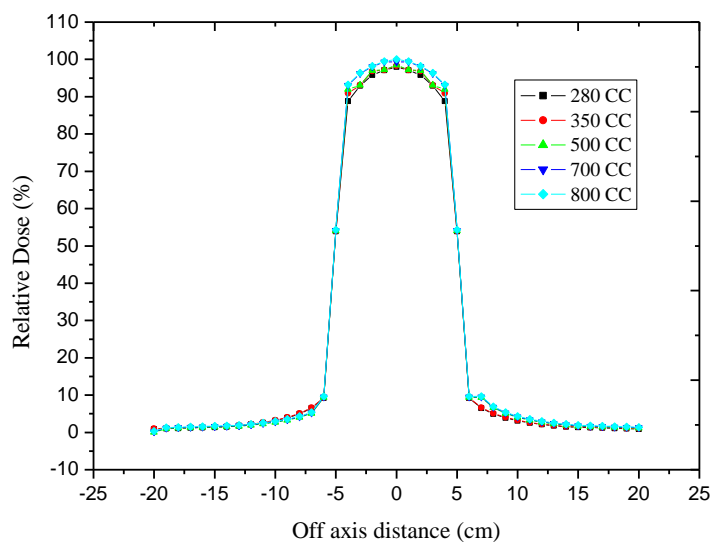
Figure 4. Comparison of measured dose profile distribution for 6 MeV photon beam with a 10×10 cm^2 field size defined at source-to-surface distance of 100 cm

Figure 4 displays the measured dose profile distribution for 6 MeV photon beam with a 10×10 cm^2 field size defined at the SSD of 100 cm. The dose profiles were measured at maximum dose (d_{max}) for different thicknesses of silicone gel prosthesis.

Monte Carlo Calculation

The effect of silicone gel thickness on dose distribution was established in this study. The water phantom was designed and modelled by the MCNP code in three-dimensions. In order to establish the accuracy of the MCNP code, the PDD curves and beam profiles obtained by means of the MCNP code were compared with the measured curves obtained from the Varian 2100C linear accelerator. The PDD curves and the dose profiles for 6 MeV photon beam as generated by the MCNP code are shown in figures below.

Validation of Monte Carlo

Figures 5 and 6 illustrate the comparison of the measured and calculated curves in water phantom. Figure 5 presents the comparison of the percentage depth doses, while figure 6 demonstrates the beam profiles at the depth of d_{max} (1.5 cm) for 6 MeV defined at a 10×10 cm^2 field size.
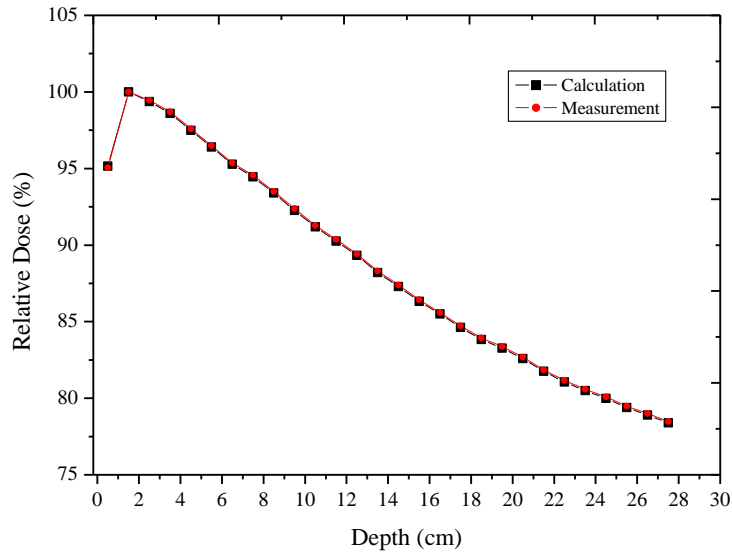
Figure   5.   Comparison   of   6   MeV   photon   beam   calculated   and   measured   in   water   for 10×10 cm^2 field size
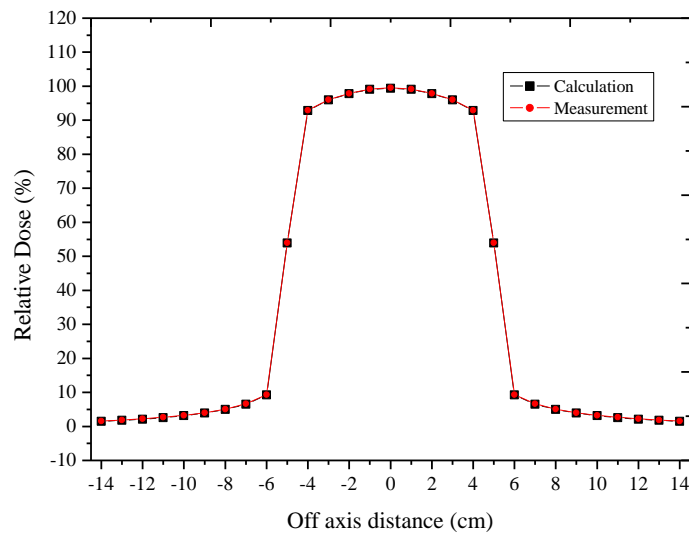
Figure 6. Comparison of measured and calculated beam profile at d_{max} in water for 6 MeV photon beam
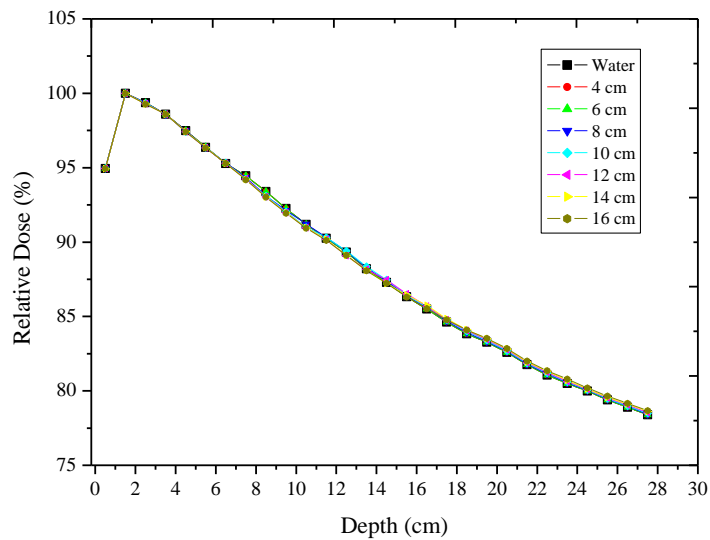
Figure 7. Comparison of calculated 6 MeV photon relative dose for various silicone gel thicknesses with a 10×10 cm^2 field size
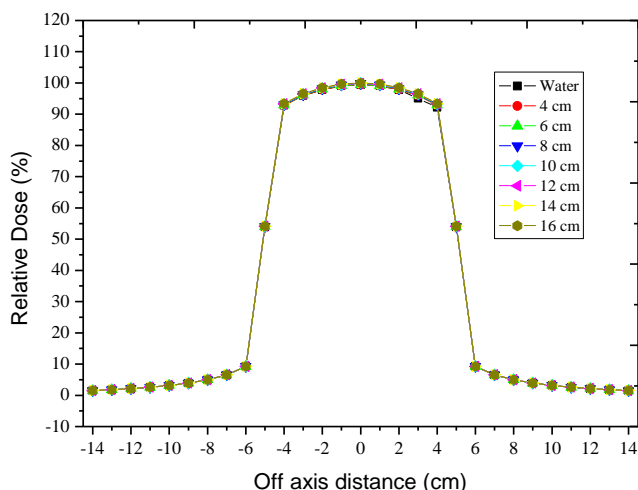
Figure 8. Beam profiles measured at d_{max} depth for various gel sizes defined at 10×10 cm² field size

Percentage depth dose

Table 1 shows the relative percentage dose calculated at 0.5 cm depth below each silicone gel thickness. The percentage differences at the depth with and without the silicone gel were also calculated.

Table 1. Relative percentage dose calculated at 0.5 cm depth below the silicone gel for 6 MeV photon beam.

Gel thickness (cm)	Without Gel	With Gel	% Diff
4	3.026	2.833	6.9
6	2.851	2.627	7.9
8	2.631	2.410	8.4
10	2.443	2.199	8.7
12	2.208	2.007	9.1
14	2.050	1.822	9.4
16	1.832	1.650	9.9

Figure 7 depicts the comparison of the calculated percentage depth dose curves for various silicone gel thicknesses, including calculations in water phantom without the silicone gel in place. The field size was defined as 10×10 cm² at the SSD of 100 cm.

Beam Profile

Figure 8 displays the comparison of the beam profiles at the depth of d_{max} for 6 MeV defined at 10×10 cm² field size.

Discussion

The simulated depth dose curves were compared to the measured depth dose curves in water (Figure 5). The calculated and the measured values of the CAX in the build-up region agreed within 1.2% for the field size of 10×10 cm² defined at 10 cm depth. There was a good relationship between the measured and simulated PDD for the 6 MeV photon beam. To validate the calculated data, gamma index between the calculated and measured data was estimated. The maximum and mean values were 1.0 at most of the depths [24].

At the build-up area a variation occurred due to the statistical noise and the difference in the measured and simulation voxel. The ratio of the measured dose to the calculated dose was 0.4 indicating the trustability of our model. The mean ratio was below 0.5, which is acceptable [25].

The results of simulation by MCNP in terms of shape and width of the dose profiles were compared with the measured dose profile. The comparison of the measured and calculated data (Figure 6) revealed a good consistency between width at 20% and 50% isodose levels; furthermore they showed 5.4% and 4.3% difference at maximum, respectively. The comparison of the data measured with values obtained by MCNP code showed a good consistency so that the highest difference observed in penumbra was less than 1 mm.

Table 1 shows the relative percentage dose calculated at the depth of 0.5 cm below the silicone gel and at the same depth in water without the silicone gel for 10×10 cm² field size. The percentage difference value for each silicone gel thickness was calculated. A slight decrease was observed in relative percentage dose with respect to the increase in silicone gel thickness.

The maximum depth dose value at 0.5 cm below the silicone gel prosthesis for all silicone gel thicknesses were calculated as 9.9%. The dose difference of approximately 8% at the interface between the prosthesis and muscle-equivalent material was obtained elsewhere [26]. The difference is believed to be due to electronic dis-equilibrium effects that occur at the interface [27]. As the silicone gel thickness was increased by 2 cm, the relative percentage dose decreased by 0.2%.

Figure 7 demonstrates the calculated dose for various silicone gel thicknesses as a function of depth. The PDD curves for 6 MeV at the field size of 10×10 cm² were plotted. The SSD was kept constant at 100 cm. The point of normalization for all depth dose curves was 100%. The slight difference observed could be attributed to the fact that silicone gel and water exhibited comparable densities and interaction range. The readings were similar due to the photon fluence entering the cross-sectional area on the first layer of water, which was the same for all geometries.

The dose reached the maximum at a depth of 1.5 cm for water and all silicone gels, which is expected of the 6 MeV photon beam. The minimal decrease in the depth dose values for photon beams with silicone gel prosthesis in place might be also due to the electron density of silicone gel (3.19×10^{23} electrons/cm^3) compared to that of water (3.34×10^{23} electron/cm^3) [28]. For the silicone gel thicknesses of 4, 6, 8, 10, 12, 14, ad 16 cm, expressed in electron/cm^3, the thicknesses were equivalent to 3.85, 5.85, 7.84, 9.85, 11.85, 13.85, and 5.85 cm of water, respectively. The calculation revealed that fewer photons were attenuated by the silicone gel as compared to those in equal thickness of water.

The cross plane profiles for 6 MeV photon beam (Figure 8) were calculated for the field size of 10×10 cm^2 in the water phantom. All beam dose profiles were normalized at 100%. The dose profile calculated across the water phantom indicated that the silicone gel built up the dose by 12.1%. As the gel thickness is increased by 2 cm, the dose decreased by 10% each time.

For calculations without the gel, the beam flatness was 0.9%, and the beam symmetry was obtained as 0%. For the calculation of the silicone gels of 14 cm, the beam flatness symmetry were 2% and 0%, respectively. Furthermore, the beam flatness and symmetry for 16 cm silicone gel were both obtained as 0%. The standard deviation varied with 0.042-0.053. The absolute relative error of 0.0003 was also obtained from the simulation. The mean ($\bar{x}$) of less than 0.1 was achieved during the simulation.

Conclusion

In the present study, Monte Carlo model, which is based on the MCNP code, was built, tested, and validated against the experimental data. We also successfully calculated the dose distribution below the silicone gel. Both simulated PDDs and beam profile data were tested against the measured data for 10×10 cm^2 field size, which were found to replicate the data within 2% and 2 mm, respectively.

Dose calculated at 0.5 cm below the silicone gel within the interface region was observed to decrease with the enhancement of silicone gel thickness. The findings revealed that the tissue around the interface region received reduced dose as compared to the delivered dose. The silicone gel thickness did not induce significant effects on dose distribution when irradiated with 6 MeV photon beams. Consequently, a 6 MeV photon beam could be used to minimize dose at the interface region.

Acknowledgment

References

1. Porter PL. Global trends in breast cancer incidence and mortality. Saluda publica de Mex. 2009; 51:141-6.
2. Hiraoka M, Mitsimori M, Shibuya K. Adjuvant radiation therapy following mastectomy for breast cancer. Breast Cancer. 2002; 9(3):190-5.
3. Stabile RJ, Santoro E, Dispaltro F, Sanfilipp LJ. Reconstructive breast surgery following mastectomy and adjunctive radiation therapy. Cancer. 1990; 45:2738-43.
4. Medline Plus Medical Encyclopaedia. Mastectomy. A service of the U.S National Library of Medicine, National Health Institutes. 2012.
5. Senkus-Konefka E, Welnicka-Jaskiewicz M, Jaskiewicz J, Jassem J. Radiotherapy for breast reconstruction or augmentation. Cancer treatment reviews. 2004; 30:671-82.
6. Rvu J, Yahalom J, Shank B, Chaglassian TA, McCormick B. Radiation therapy after breast augmentation or reconstruction in early or recurrent breast cancer. Cancer. 1990; 66:844-7.
7. Bostwick III J. Beast reconstruction following mastectomy. C A cancer J Clic. 1995; 45:289-304.
8. Stevanovic O, Jakovljevic. Imaging of the Breast-the efficiency for breast cancer follow-up after conserving therapy and breast implant following mastectomy. Archive of Oncology. 2001; 9:85.
9. Park AJ, Watson AC. Silicone gel breast implants, breast cancer and connective tissue disorder. Br J Surg. 1993; 80(9):1097-100.
10. Silverman BG, Brown SL, Bright RA, Kaczmarek RG, Arrowsmith-Lowe JB, Kessler DA. Reported complications of silicone gel breast implants: an epidemiologic review. Annals of internal medicine. 1996 Apr 15; 124(8):744-56.
11. Noone RB, Frazier TG, Noone GC, Blanchet NP, Murphy JB, Rose D. Recurrence of Breast Carcinoma following immediate Reconstruction: a 13-year review. Plastic Reconstr Surg. 1994; 93:96-106.
12. Shedbalkar AR, Devata A, Padanilam T. A study of effects of radiation on silicone prostheses. Plastic Reconstr Surg. 1980; 65:805-10.
13. Klein EE, Kuske RR. Changes in photon dose distributions due to breast prosthesis. Int J Radiat Oncl Biol Phys. 1993; 25:541-9.
14. Piontek RW, Kase KR. Radiation Transmission Study of Silicone Elastomer for Mammary prosthesis. Radiology. 1980; 136:505-7.
15. Krishnan L, Krishnan EC. Electron beam irradiation after irradiation reconstruction with silicone gel implant in breast cancer. Am J Clinical Oncol. 1986; 9:223-6.
16. Roberts R. How accurate is a CT-based dose calculation on a pencil beam TPS for a patient with metallic prosthesis? Phys. Med. Biol. 2001; 46:227-34.
17. Letsoalo W. The effect of sizes of silicone gel breast prosthesis on the photon beam dose distribution. Thesis. 2012.

18. Shultis JK, Faw RE. An MCNP Primer. Department of Mechanical and Nuclear Engineering, Kansas State University, Manhattan, KS 66506. 2011.

19. Shin-Etsu. Last accessed 24 November 2012. Available from: Http://www.shinetsu.com.

20. Bondurant S, Enerste V, Herdman R. Textbook of Safety of Silicone Breast Implants. National Academy Press (US) Washington D.C. 1999.

21. Adams W.P. Jr. History of Breast Implants - I. Last accessed 2012. Available from: Http://dr-adams.com.

22. Keall P, Siebers JV, Libby B, Mohan R. Determining the incident electron fluence for Monte Carlo based photon treatment planning using standard measured data set. Med Phys. 2003; 30:574-82.

23. Cho SH, Vassiliev ON, Lee S, Liu HH, Ibbott GS, Mohan R. Reference photon dosimetry data and reference phase space data for the 6 MV photon beam from Varian Clinic 2100 series linear accelerator. Med Phys. 2005; 32:137-48.

24. Aghdam MR, Baghani HR, Mahdavi SR, Akbari ME. Monte Carlo study on effective source to surface distance for electron beams from a mobile dedicated IORT accelerator. Journal of Radiotherapy in Practice. 2017 Mar; 16(1):29-37.

25. Jiang SB, Kapur A, Ma C-M. Electron beam modelling and commissioning for Monte Carlo treatment planning. Med Phys. 2000; 27:180-91.

26. McGinley PH, Powell WR, Bostwick J. Dosimetry of silicone breast prosthesis. Radiology. 1980; 135:223-4.

27. Pradhan AS, Gopala KK, Iyer PS. Dose measurement at high atomic number interfaces in megavoltage photon beams using TLDs. Med Phys. 1992; 19:355-6.

28. Krishnan L, St George FJ, Mansfield CM, Krishnan EC. Effect of Silicone gel breast prosthesis on electron and photon dose distributions. Med Phys. 1983; 10:96-9.